# Network-Level Assessment of Motorway Pavement Using the Traffic Speed Deflectometer

Andrea Graziani, a.graziani@univpm.it

3rd SIIV International Winter School
December 18th-21st, 2022 - Moena

Pavement Assessment and management towards Smart and Safer mobility

PDF created on 2022-12-19, 14:28

# Outline

# Outline

# Pavement asset management

Every year road Authorities (ANAS, ASPI, DRD, MnDOT...) invest billions of euro for providing and managing pavement assets that meet legislative and public expectations

# Pavement asset management

Every year road Authorities (ANAS, ASPI, DRD, MnDOT...) invest billions of euro for providing and managing pavement assets that meet legislative and public expectations

Within an asset management, context they rely on a Pavement Management System (PMS) to assists transportation executives and chief engineers in allocating their funds in an optimal way (Haas and Hudson, 2015)

# Pavement asset management

Every year road Authorities (ANAS, ASPI, DRD, MnDOT...) invest billions of euro for providing and managing pavement assets that meet legislative and public expectations

Within an asset management, context they rely on a Pavement Management System (PMS) to assists transportation executives and chief engineers in allocating their funds in an optimal way (Haas and Hudson, 2015)

At the network-level, the entire pavement network (thousands of kilometres) is divided in sections and each pavement section is evaluated using condition indices or scores which are physically meaningful and do not require extensive testing and evaluation efforts

# Pavement condition indices

We may identify surface distress indices (e.g. PCI), roughness indices (e.g. IRI) and skid resistance indices (e.g. IFI) as key performance indicators (KPI) for the comfort and safety of the road users

For guiding rehabilitation decisions and budget projection is structural capacity (*aka* structural adequacy, bearing capacity, strength, structural strength. . . ), is the most important indicator

# Pavement condition indices

We may identify surface distress indices (e.g. PCI), roughness indices (e.g. IRI) and skid resistance indices (e.g. IFI) as key performance indicators (KPI) for the comfort and safety of the road users

For guiding rehabilitation decisions and budget projection is structural capacity (*aka* structural adequacy, bearing capacity, strength, structural strength. . . ), is the most important indicator

Structural capacity is estimated using nondestructive deflection testing (NDT)

$\Rightarrow$ The deflection of a pavement surface resulting from an applied load is considered to be an indicator of the rate at which pavement deterioration will occur under traffic

# NDT at the network-level

Nowadays, the device most commonly used for NDT is the falling weigth deflectometer (FWD)

The FWD is en excellent tool for project-level where sophisticated structural analysis is needed.

# NDT at the network-level

Nowadays, the device most commonly used for NDT is the falling weigth deflectometer (FWD)

The FWD is en excellent tool for project-level where sophisticated structural analysis is needed.

At the network-level, operation of the FWD is limited because the test method is slow and creates traffic disruption and hazard

Equipments that measure pavement deflections continously, while moving at traffic speed are now available. The most widely used is the traffic speed deflectometer (TSD)

# Outline

# The TSD vehichle

# The measuring equipment (4th generation)

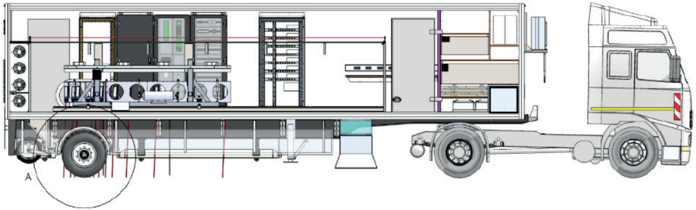

# The measuring equipment (4th generation)

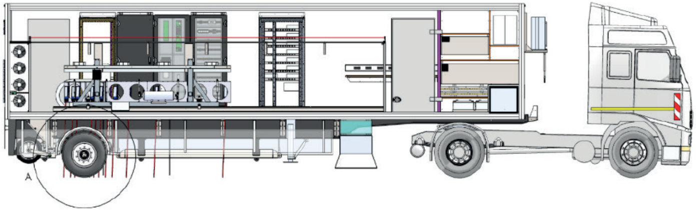


50+50 kN load applied on rear dual-tyred single axle

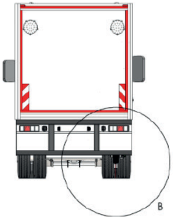

# The measuring equipment (4th generation)

50+50 kN load applied on rear dual-tyred single axle

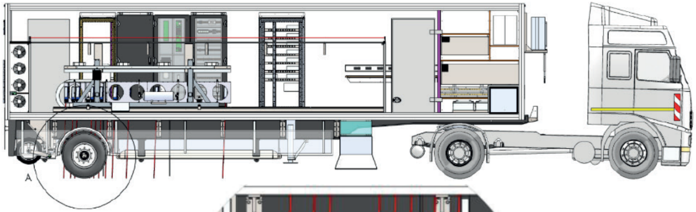


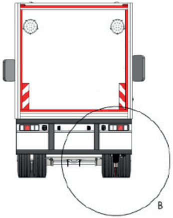


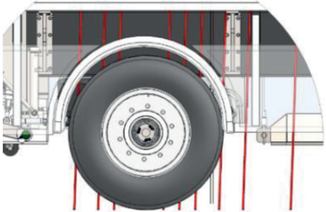

11 laser Doppler sensors positioned at different distances from the load (both in front and behind)

# The measuring equipment (4th generation)

50+50 kN load applied on rear dual-tyred single axle

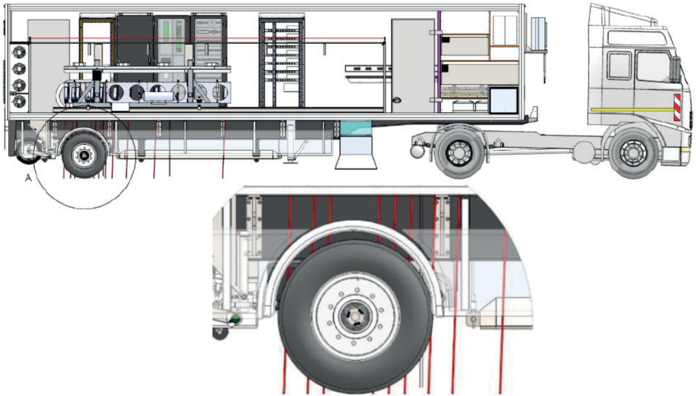


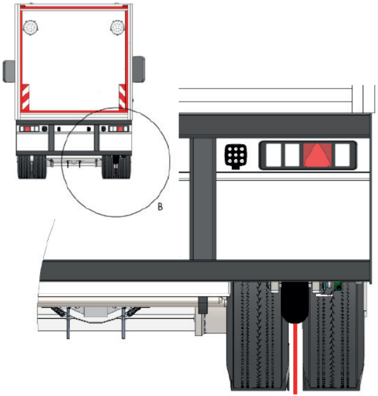


11 laser Doppler sensors positioned at different distances from the load (both in front and behind)

All sensors are aligned in a single wheelpath

# The measuring equipment (4th generation)

Additional equipment include: odometer, inertial refernce, temperatue conditioning for the sensors (20 °C)

50+50 kN load applied on rear dual-tyred single axle

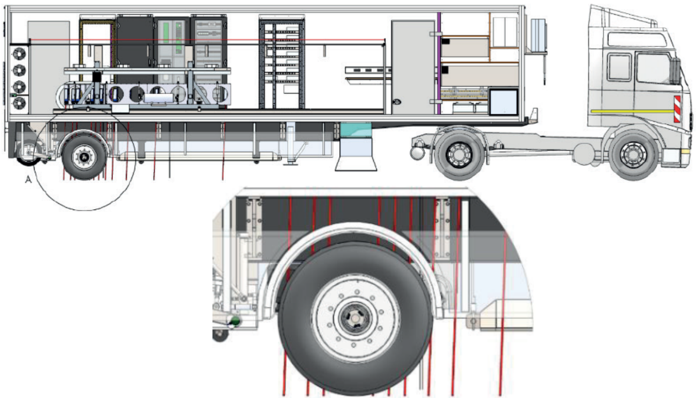


11 laser Doppler sensors positioned at different distances from the load (both in front and behind)

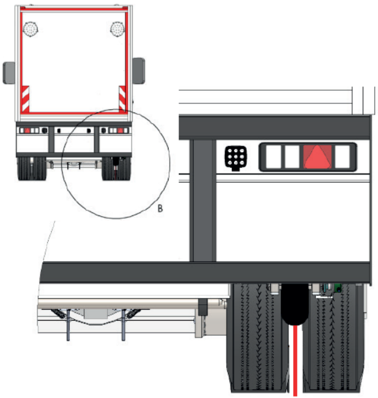


All sensors are aligned in a single wheelpath

# Surface deflection slope

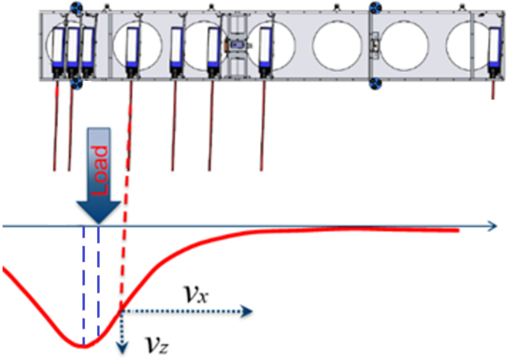


Laser Doppler sensors measure the vertical displacement velocity ($v_z$) of the pavement surface due to the applied load

# Surface deflection slope

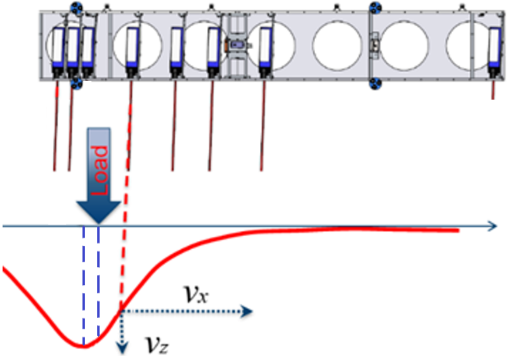


Laser Doppler sensors measure the vertical displacement velocity ($v_z$) of the pavement surface due to the applied load

Horizontal displacement velocity ($v_x$) is equal to the vehicle speed

Surface deflection slope $z'(x)$ is the measurement output of the TSD:

$$\frac{v_z}{v_x} = \frac{\mathrm{d}z/\mathrm{d}t}{\mathrm{d}x/\mathrm{d}t} = \frac{\mathrm{d}z}{\mathrm{d}x} = z'(x)$$

# Surface deflection slope

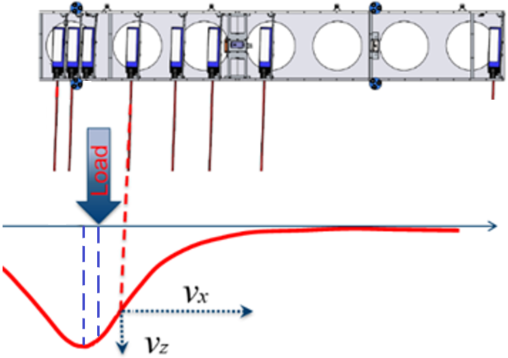


Laser Doppler sensors measure the vertical displacement velocity ($v_z$) of the pavement surface due to the applied load

Horizontal displacement velocity ($v_x$) is equal to the vehicle speed

Surface deflection slope $z'(x)$ is the measurement output of the TSD:

$$\frac{v_z}{v_x} = \frac{\mathrm{d}z/\mathrm{d}t}{\mathrm{d}x/\mathrm{d}t} = \frac{\mathrm{d}z}{\mathrm{d}x} = z'(x)$$

Note 1: lasers are at an angle of about 2°, to allow removing the effect of the suspension movement

Note 2: the maximum deflection is not located directly beneath the load (viscoelastic effect)

# Surface deflection

Surface deflection is obtained by integrating the deflection slope: $z(x) = \int_x^\infty z'(y)\,\mathrm{d}y$

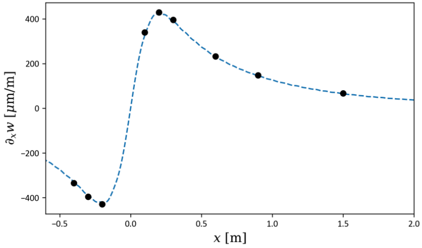


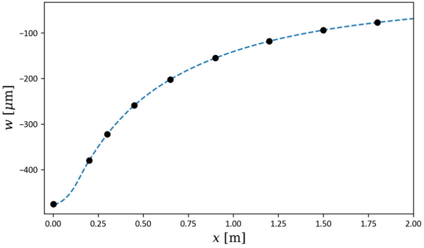

Surface deflection is obtained by integrating the deflection slope: $z(x) = \int_x^{\infty} z'(y)\,\mathrm{d}y$

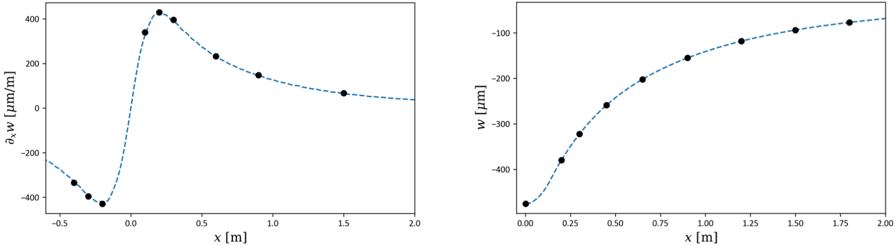


Before integrating, a "continuous" deflection slope profile is fitted on the measured data using regression/interpolation (Dias et al., 2005; Nielsen, 2019; Pedersen, 2013)(Muller and Roberts, 2013; Zofka et al., 2014)

# TSD operation

GREENWOOD
ENGINEERING

# Recording, reporting and analysing data

Deflection slope data are collected almost continuously. The laser sampling rate is about 1 kHz, at a vehicle speed of about 20 m/s (72 km/h) this corresponds to a ore reading every 20 mm

This data rate is too high and for most practical purpose. Therefore, data are averaged over lengths of 1 m or 10 m

# Recording, reporting and analysing data

Deflection slope data are collected almost continuously. The laser sampling rate is about 1 kHz, at a vehicle speed of about 20 m/s (72 km/h) this corresponds to a ore reading every 20 mm

This data rate is too high and for most practical purpose. Therefore, data are averaged over lengths of 1 m or 10 m

For pavement network-level management a further data aggregation ("pavement section") is necessary (Rada et al., 2016)

- The optimum aggregation interval is controlled by the size of the network to be tested and practices of local highway agencies (e.g 150 m, 250 m, 500 m)
- statistical processing of the data is needed so that with minimal volume of data the significant areas with structural defect could be identified

# Sample output file

| | A | B | C | D | E | F |
|---|---|---|---|---|---|---|
| 1 | Distance [m] | Speed [Km/h] | Applied Load - Left [Kg] | Applied Load - RIght [Kg] | Air Temperature [deg C] | Surface Temperature [deg C] |
| 2 | 0 | 23.9568 | 4282.7298 | 6324.2173 | 25.71 | 31.15 |
| 3 | 10 | 23.9054 | 4341.3683 | 6318.9825 | 25.7 | 31.2 |
| 4 | 20 | 23.8442 | 4205.0945 | 6322.1242 | 25.69 | 31.21 |

TSDsurvey

# Sample output file

| | A | B | C | D | E | F |
|---|---|---|---|---|---|---|
| 1 | Distance [m] | Speed [Km/h] | Applied Load - Left [Kg] | Applied Load - RIght [Kg] | Air Temperature [deg C] | Surface Temperature [deg C] |
| 2 | 0 | 23.9568 | 4282.7298 | 6324.2173 | 25.71 | 31.15 |
| 3 | 10 | 23.9054 | 4341.3683 | 6318.9825 | 25.7 | 31.2 |
| 4 | 20 | 23.8442 | 4205.0945 | 6322.1242 | 25.69 | 31.21 |

| | G | H | I | J | K | L | M | N | O | P |
|---|---|---|---|---|---|---|---|---|---|---|
| 1 | SCI300 [Âµm] | D(0)[Âµm] | D(100)[Âµm] | D(200)[Âµm] | D(300)[Âµm] | D(400)[Âµm] | D(500)[Âµm] | D(600)[Âµm] | D(700)[Âµm] | D(800)[Âµm] |
| 2 | | | | | | | | | | |
| 3 | 22 | -75 | -66 | -56 | -54 | -52 | -51 | -50 | -48 | -46 |
| 4 | 25 | -75 | -65 | -53 | -50 | -49 | -48 | -46 | -45 | -44 |

TSDsurvey

# Sample output file

| | A | B | C | D | E | F |
|---|---|---|---|---|---|---|
| 1 | Distance [m] | Speed [Km/h] | Applied Load - Left [Kg] | Applied Load - RIght [Kg] | Air Temperature [deg C] | Surface Temperature [deg C] |
| 2 | 0 | 23.9568 | 4282.7298 | 6324.2173 | 25.71 | 31.15 |
| 3 | 10 | 23.9054 | 4341.3683 | 6318.9825 | 25.7 | 31.2 |
| 4 | 20 | 23.8442 | 4205.0945 | 6322.1242 | 25.69 | 31.21 |

| | G | H | I | J | K | L | M | N | O | P |
|---|---|---|---|---|---|---|---|---|---|---|
| 1 | SCI300 [Âµm] | D(0)[Âµm] | D(100)[Âµm] | D(200)[Âµm] | D(300)[Âµm] | D(400)[Âµm] | D(500)[Âµm] | D(600)[Âµm] | D(700)[Âµm] | D(800)[Âµm] |
| 2 | | | | | | | | | | |
| 3 | 22 | -75 | -66 | -56 | -54 | -52 | -51 | -50 | -48 | -46 |
| 4 | 25 | -75 | -65 | -53 | -50 | -49 | -48 | -46 | -45 | -44 |

| | Q | R | S | T | U | V | W | X | Y | Z |
|---|---|---|---|---|---|---|---|---|---|---|
| 1 | D(900)[Âµm] | D(1000)[Âµm] | D(1100)[Âµm] | D(1200)[Âµm] | D(1300)[Âµm] | D(1400)[Âµm] | D(1500)[Âµm] | D(1600)[Âµm] | D(1700)[Âµm] | D(1800)[Âµm] |
| 2 | | | | | | | | | | |
| 3 | -45 | -43 | -41 | -39 | -36 | -34 | -32 | -30 | -29 | -27 |
| 4 | -42 | -40 | -39 | -37 | -35 | -33 | -31 | -30 | -28 | -26 |

TSDsurvey

# Sample output file

| | A | B | C | D | E | F |
|---|---|---|---|---|---|---|
| 1 | Distance [m] | Speed [Km/h] | Applied Load - Left [Kg] | Applied Load - RIght [Kg] | Air Temperature [deg C] | Surface Temperature [deg C] |
| 2 | 0 | 23.9568 | 4282.7298 | 6324.2173 | 25.71 | 31.15 |
| 3 | 10 | 23.9054 | 4341.3683 | 6318.9825 | 25.7 | 31.2 |
| 4 | 20 | 23.8442 | 4205.0945 | 6322.1242 | 25.69 | 31.21 |

| | G | H | I | J | K | L | M | N | O | P |
|---|---|---|---|---|---|---|---|---|---|---|
| 1 | SCI300 [Âµm] | D(0)[Âµm] | D(100)[Âµm] | D(200)[Âµm] | D(300)[Âµm] | D(400)[Âµm] | D(500)[Âµm] | D(600)[Âµm] | D(700)[Âµm] | D(800)[Âµm] |
| 2 | | | | | | | | | | |
| 3 | 22 | -75 | -66 | -56 | -54 | -52 | -51 | -50 | -48 | -46 |
| 4 | 25 | -75 | -65 | -53 | -50 | -49 | -48 | -46 | -45 | -44 |

| | Q | R | S | T | U | V | W | X | Y | Z |
|---|---|---|---|---|---|---|---|---|---|---|
| 1 | D(900)[Âµm] | D(1000)[Âµm] | D(1100)[Âµm] | D(1200)[Âµm] | D(1300)[Âµm] | D(1400)[Âµm] | D(1500)[Âµm] | D(1600)[Âµm] | D(1700)[Âµm] | D(1800)[Âµm] |
| 2 | | | | | | | | | | |
| 3 | -45 | -43 | -41 | -39 | -36 | -34 | -32 | -30 | -29 | -27 |
| 4 | -42 | -40 | -39 | -37 | -35 | -33 | -31 | -30 | -28 | -26 |

| | AA | AB | AC |
|---|---|---|---|
| 1 | Latitude [decimal degrees] | Longitude [decimal degrees] | Altitude [m] |
| 2 | 44.35763862 | 11.80330102 | 30.856 |
| 3 | 44.35760181 | 11.80341641 | 30.856 |
| 4 | 44.35756506 | 11.80353138 | 30.856 |

TSDsurvey

# Structural capacity: the SCI300

Surface Curvature Index $SCI300$:

$$SCI300 = D(300) - D(0)$$

| | G | H | I | J | K |
|---|---|---|---|---|---|
| 1 | SCI300 [Âµm] | D(0)[Âµm] | D(100)[Âµm] | D(200)[Âµm] | D(300)[Âµm] |
| 2 | | | | | |
| 3 | 22 | -75 | -66 | -56 | -54 |
| 4 | 25 | -75 | -65 | -53 | -50 |

# Structural capacity: the SCI300

Surface Curvature Index $SCI300$:

$$SCI300 = D(300) - D(0)$$

| | G | H | I | J | K |
|---|---|---|---|---|---|
| 1 | SCI300 [Âµm] | D(0)[Âµm] | D(100)[Âµm] | D(200)[Âµm] | D(300)[Âµm] |
| 2 | | | | | |
| 3 | 22 | -75 | -66 | -56 | -54 |
| 4 | 25 | -75 | -65 | -53 | -50 |

Routinely used in Europe, it correlates to the horizontal deformation at the bottom of the bituminous layers, an indicator of fatigue cracking

$$\varepsilon_{bottom} = 0.481 + 0.881 \log(SCI300)$$

SCI300 obtained from FWD (Molenaar, 2007)

# Structural capacity: the SCI300

Surface Curvature Index $SCI300$:

$$SCI300 = D(300) - D(0)$$

| | G | H | I | J | K |
|---|---|---|---|---|---|
| 1 | SCI300 [Âµm] | D(0)[Âµm] | D(100)[Âµm] | D(200)[Âµm] | D(300)[Âµm] |
| 2 | | | | | |
| 3 | 22 | -75 | -66 | -56 | -54 |
| 4 | 25 | -75 | -65 | -53 | -50 |

Routinely used in Europe, it correlates to the horizontal deformation at the bottom of the bituminous layers, an indicator of fatigue cracking

$$\varepsilon_{bottom} = 0.481 + 0.881 \log(SCI300)$$

SCI300 obtained from FWD (Molenaar, 2007)

Several other indices may be used, Rada et al., 2016 and Nasimifar et al., 2016 present a comprehensive study based on viscoelastic simulations (3D move), focusing on TSD-based indices (not FWD-based...)

# Outline

# Literature review topics

Development of the TSD (historical note)

Comparing TSD and FWD measurements

Applying TSD measurements for network-level pavement management

# Early development of the TSD

First prototype: "High Speed Deflectograph" (one laser) developed between 1996 and 2001 (Hildebrand and Rasmussen, 2002) from a collaboration between DRD and Greenwood

# Early development of the TSD

First prototype: "High Speed Deflectograph" (one laser) developed between 1996 and 2001 (Hildebrand and Rasmussen, 2002) from a collaboration between DRD and Greenwood

The "1st generation" TSD (four lasers) operated from 2005 on the Danish state road network (Baltzer, 2009; Rasmussen et al., 2008) and in the UK (Ferne et al., 2009a, 2009b)

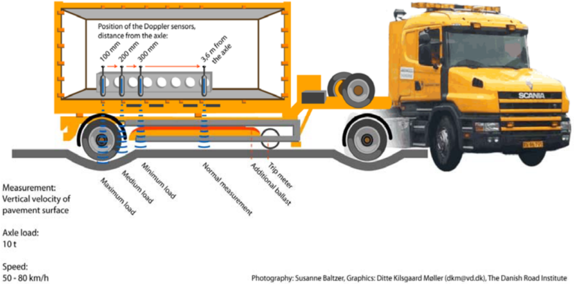

# Early results with the TSD

Measurements were repeatable in the short-term (consecutive TSD passes) whereas, on the long-term, were affected by pavement degradation and temperature (year-to-year variability)

It was possible to distinguish between "weak" and "strong" pavements

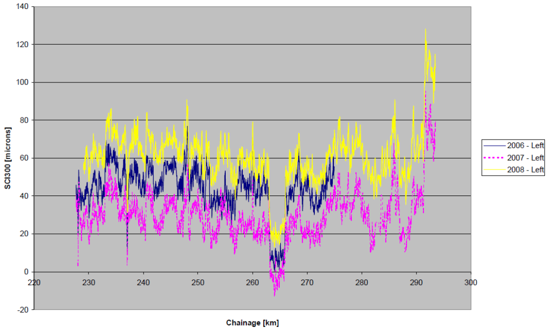


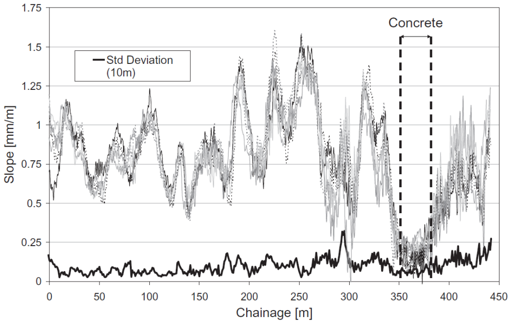

# Early results with the TSD

Measurement quality (valid data) was affected by surface condition, with lowest quality on dark/wet/distressed pavements

Calibration is necessary for correcting the inevitable lack of precise alignment of the measuring and reference lasers

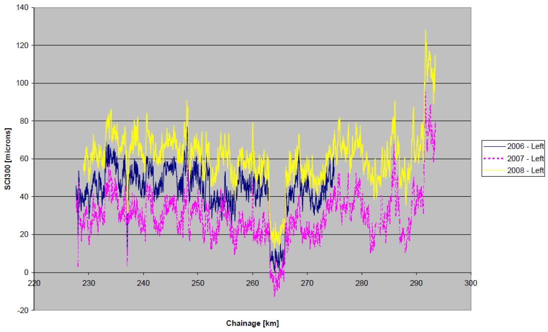


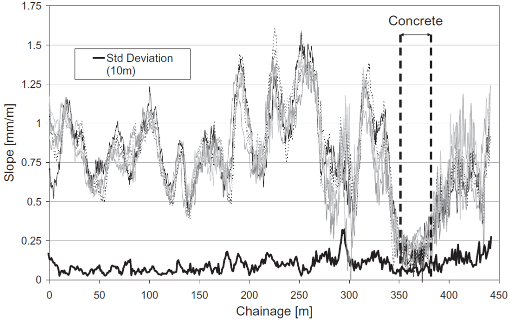

# Outside Europe: Australia

In 2010, the first TSD was shipped to Australia and tested on 18.000 km of pavements in New South Wales and Queensland (Kelley and Moffat, 2012; Roberts et al., 2014)

Most tests were carried out on low-volume pavements (granular pavements with a thin layer of sprayed bitumen and chip seal )

# Outside Europe: Australia

In 2010, the first TSD was shipped to Australia and tested on 18.000 km of pavements in New South Wales and Queensland (Kelley and Moffat, 2012; Roberts et al., 2014)

Most tests were carried out on low-volume pavements (granular pavements with a thin layer of sprayed bitumen and chip seal )

Results confirmed the correlation between the maximum deflection measured by FWD and TSD (deflections ranged from approximately 100 to 2000 microns), but highlighted that the correlation was pavement-specific

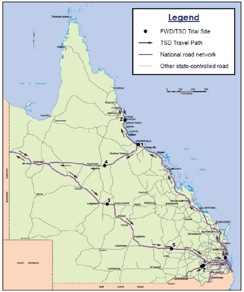


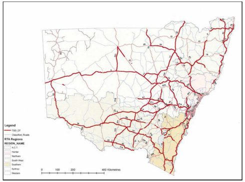

# Outside Europe: United States

The FHWA sponsored a project (2012–2015) aimed at evaluating the TSD and the Rolling Wheel Deflectometer (a similar equipment) for pavement structural evaluation at the network level (Rada et al., 2016)

The project involved field trials performed mainly on the MnROAD facility stresses, strains, and surface deflections were measured and correlated to TSD/RWD output

Results confirmed that both devices were capable of providing reasonably accurate and precise pavement response measurements

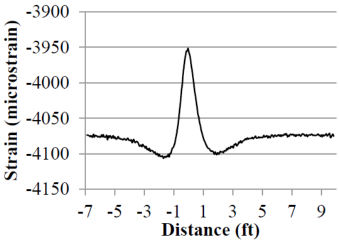


Figure 40. Graph. MnROAD strain gauge reduced data.

Figure 27. Photo. Grooving of pavement for sensor installation.

# Comparing TSD and FWD measurements

Obtaining a correlation or at least quantifying the agreement between the deflections measured by the devices would allow to combine the datasets and analyse them jointly

# Comparing TSD and FWD measurements

Obtaining a correlation or at least quantifying the agreement between the deflections measured by the devices would allow to combine the datasets and analyse them jointly

Obvious differences between the FWD- and TSD-measured deflections are due to:

- shape and dimension of loading area (circular plate Vs dual tyre)
- measuring mode (stationary Vs moving)
- deflection basin calculation (direct Vs indirect)

# Comparing TSD and FWD measurements

Obtaining a correlation or at least quantifying the agreement between the deflections measured by the devices would allow to combine the datasets and analyse them jointly

Obvious differences between the FWD- and TSD-measured deflections are due to:

- shape and dimension of loading area (circular plate Vs dual tyre)
- measuring mode (stationary Vs moving)
- deflection basin calculation (direct Vs indirect)

Several researchers have tackled this problem starting from the fact that both FWD and TSD measurements are affected by uncertainty(they do not provide "true values") and thus a simple regression approach (least-squares) is not correct

# Comparing TSD and FWD measurements

Katicha et al., 2014 used the limits of agreement (LOA) method (Bland and Altman, 1986) to compare SCI300 and BDI values obtained with TSD and FWD

Levenberg et al., 2018 converted SCI300 values from the FWD into corresponding "TSD300" values and than used a modern agreement metrics ($\lambda$) that summarizes the closeness of two datasets in a single index, considering both correlation and bias

Bodin et al., 2019 used Deming regression that considers that both sets of data are measured with errors, and is often employed in comparing the data outputs of two measurement methods

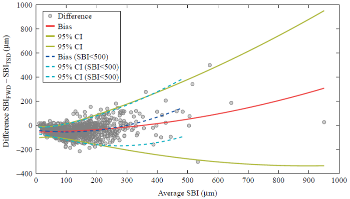


| TSD Run # | Speed [km/h] | Agreement ranking based on $\lambda$ | Agreement ranking based on $r$ |
|---|---|---|---|
| 4 | 40 | 5 | 6 |
| | 60 | 6 | 4 |
| | 70 | 3 | 1 |
| 5 | 40 | 4 | 5 |
| | 60 | 1 | 3 |
| | 70 | 2 | 2 |

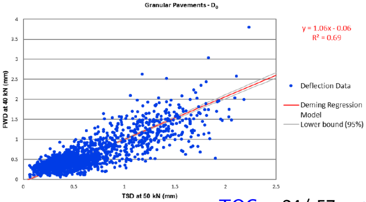

# TSD for network-level management: the Danish approach

The Danish Road Directorate (DRD) sponsored the TSD development and has a long-time experience in its use for network-level management

# TSD for network-level management: the Danish approach

The Danish Road Directorate (DRD) sponsored the TSD development and has a long-time experience in its use for network-level management

According to the DRD approach, the SCI300 values, reported with a 10 m interval, are compared with the following thresholds

$$\text{Threshold 1 } (\mu\text{m}) = 600 \times N^{-\log 2}$$
$$\text{Threshold 2 } (\mu\text{m}) = 900 \times N^{-\log 2}$$

N = daily traffic in 100 kN-ESALs

When the SCI300 values are lower than Threshold 1, the pavement is considered in good structural condition

Conversely, when the SCI300 values exceed Threshold 2, additional investigations at the project level are deemed necessary (e.g. with the FWD)

# TSD for network-level management: recent developments

Shrestha et al., 2018 analysed the results of a pooled found study involving 9 State Highway Agencies. They developed SCI300 thresholds based on residual fatigue resistance and expected traffic for Virginia pavements

# TSD for network-level management: recent developments

Shrestha et al., 2018 analysed the results of a pooled found study involving 9 State Highway Agencies. They developed SCI300 thresholds based on residual fatigue resistance and expected traffic for Virginia pavements

Zihan et al., 2018, 2019 analysed the results of a Louisiana study to calculate a TSD-based effective Structural Number ($SN_{eff}$) and compared to FWD-based $SN_{eff}$

# TSD for network-level management: recent developments

Shrestha et al., 2018 analysed the results of a pooled found study involving 9 State Highway Agencies. They developed SCI300 thresholds based on residual fatigue resistance and expected traffic for Virginia pavements

Zihan et al., 2018, 2019 analysed the results of a Louisiana study to calculate a TSD-based effective Structural Number ($SN_{eff}$) and compared to FWD-based $SN_{eff}$

Nasimifar et al., 2019 analysed the results of the FHWA study to calculate a TSD-based effective Structural Number ($SN_{eff}$) and compared to FWD-based $SN_{eff}$

# TSD for network-level management: recent developments

Shrestha et al., 2018 analysed the results of a pooled found study involving 9 State Highway Agencies. They developed SCI300 thresholds based on residual fatigue resistance and expected traffic for Virginia pavements

Zihan et al., 2018, 2019 analysed the results of a Louisiana study to calculate a TSD-based effective Structural Number ($SN_{eff}$) and compared to FWD-based $SN_{eff}$

Nasimifar et al., 2019 analysed the results of the FHWA study to calculate a TSD-based effective Structural Number ($SN_{eff}$) and compared to FWD-based $SN_{eff}$

Pettinari et al., 2021 analysed the results of a joint study between DRD and German BASt to estimate remaining life (in ESALs) starting from correlation between TSD-based and FWD-based SCI300 values

. . .

# Outline

# TSD survey on the ASPI network

The survey was part of the UNIVPM research project HiPER sponsored by Autostrade per l'Italia (ASPI)

Results of the HiPER project have been used by Movyon for developing the Evolutive Pavement Management System (E-PMS) for the ASPI motorway network (Chiola et al., 2022)

# The investigated network

About 400 km of dual-carriageway motorway pavement located around the city of Bologna

# The investigated network

| Branch ID | Starting position [km] | Ending position [km] | Length [km] | Lanes (*) | Traffic [ESAL/year] |
|---|---|---|---|---|---|
| B1a | 119 + 500 | 155 + 500 | 36.0 | 3 | $16.4 \cdot 10^6$ |
| B1b | 155 + 500 | 188 + 900 | 33.4 | 4 | $16.4 \cdot 10^6$ |
| B2 | 210 + 100 | 220 + 000 | 9.9 | 2 | $10.1 \cdot 10^6$ |
| B3 | 56 + 700 | 143 + 900 | 87.2 | 3 | $9.1 \cdot 10^6$ |
| B4 | 0 + 000 | 29 + 800 | 29.8 | 2 | $2.2 \cdot 10^6$ |

(*) in each carriageway. Both carriageways/directions were surveyed.

Only the right lane of each carriageway was surveyed because it is the most affected by heavy traffic

- Branches B1, B3 and B4 have the typical semi-rigid pavement structure of Italian motorways:
  - 29 cm of asphalt concrete (including 4 cm of OGFC)
  - 25 cm of cement-treated subbase
  - granular subbase of variable thickness (depending on subgrade)
- the OGFC is not present on branch B2 (mountainous terrain)

# Summary of TSD measurements

TSD 7 (4th generation, 11 lasers) operated by Greenwood, from 16 to 18 June 2020

- Target speed was 80 km/h
- Output files with reporting intervals of 10 m and 1 m ⏩ Output file (1m)
- The load applied on the right wheels of the loading axle was always greater than that applied on the left wheels (the average values were 62 and 43 kN, respectively)
- Air temperature $T_{air} = 20 - 30\ ^{\circ}\mathrm{C}$, Pavement surface temperature $T_{pav} = 23 - 36\ ^{\circ}\mathrm{C}$
- 40 and 80 % of valid data (i.e. data actually reported at the measurement points)
  - Invalid data may be due to the characteristics of the pavement surface (e.g. excessively uneven or wet) or to the incorrect operation of the TSD equipment (e.g. in the presence of construction sites, bridges/viaducts or in the case of overtaking of heavy vehicles)

# SCI300 on B1 and B4

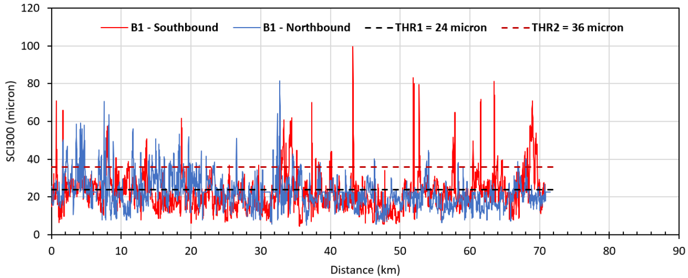


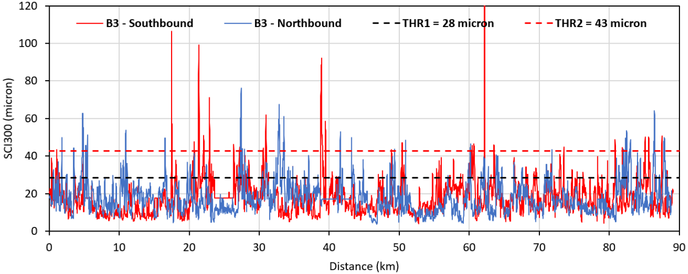

# SCI300 summary (entire surveyed network)

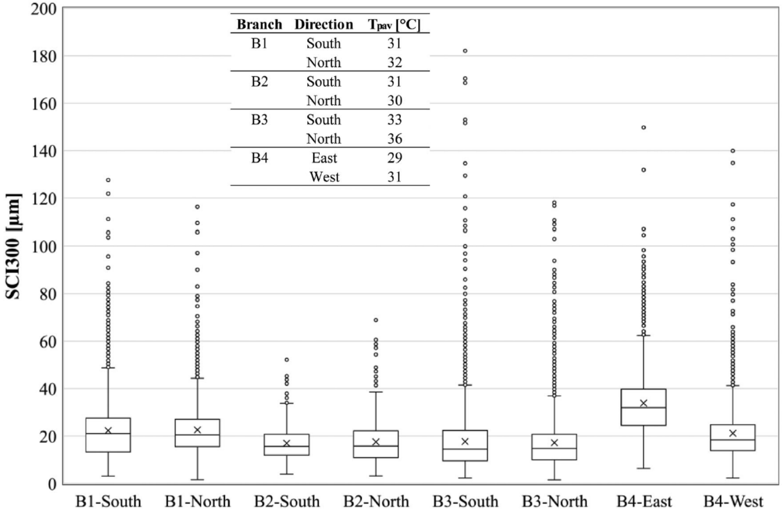

# Difference between B1a and B1b

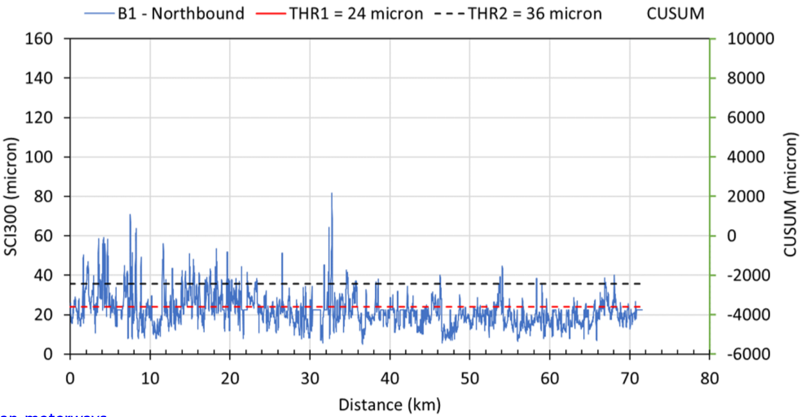

$$\textbf{CUSUM} = \sum_{i=1}^{n} (SCI300_i - \overline{SCI300})$$

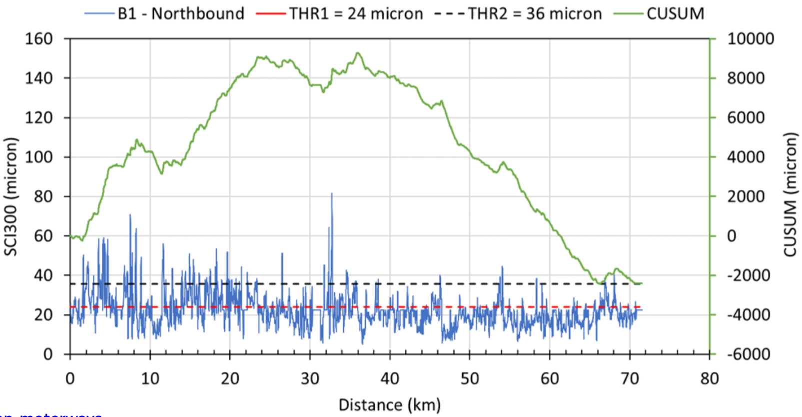

# Difference between B1a and B1b

$$\textbf{CUSUM} = \sum_{i=1}^{n} (SCI300_i - \overline{SCI300})$$

Positive slope: SCI300 above average

Negative slope: SCI300 below average

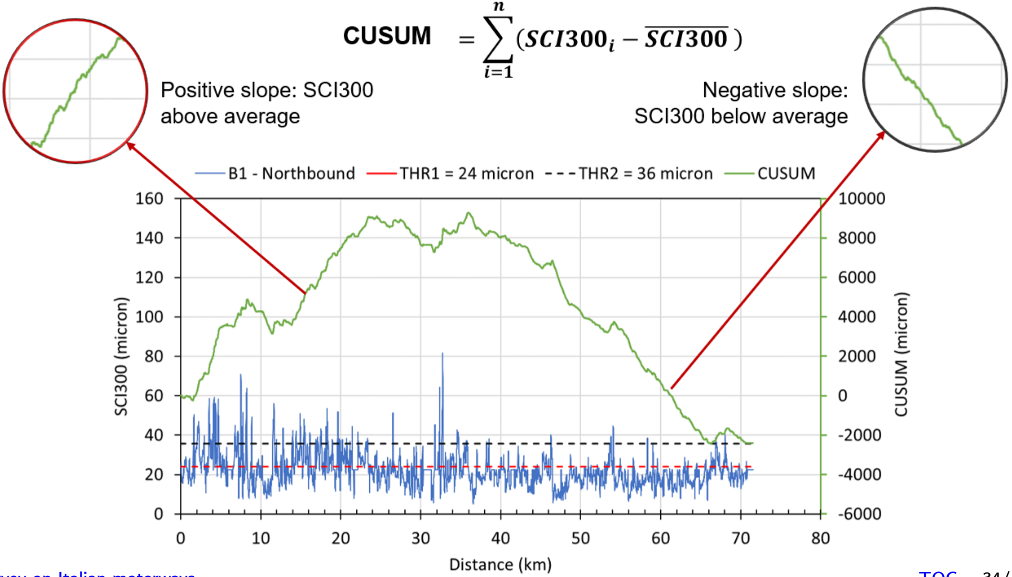

# Difference between B1a and B1b

$$\textbf{CUSUM} = \sum_{i=1}^{n} (SCI300_i - \overline{SCI300})$$

Positive slope: SCI300 above average

Negative slope: SCI300 below average

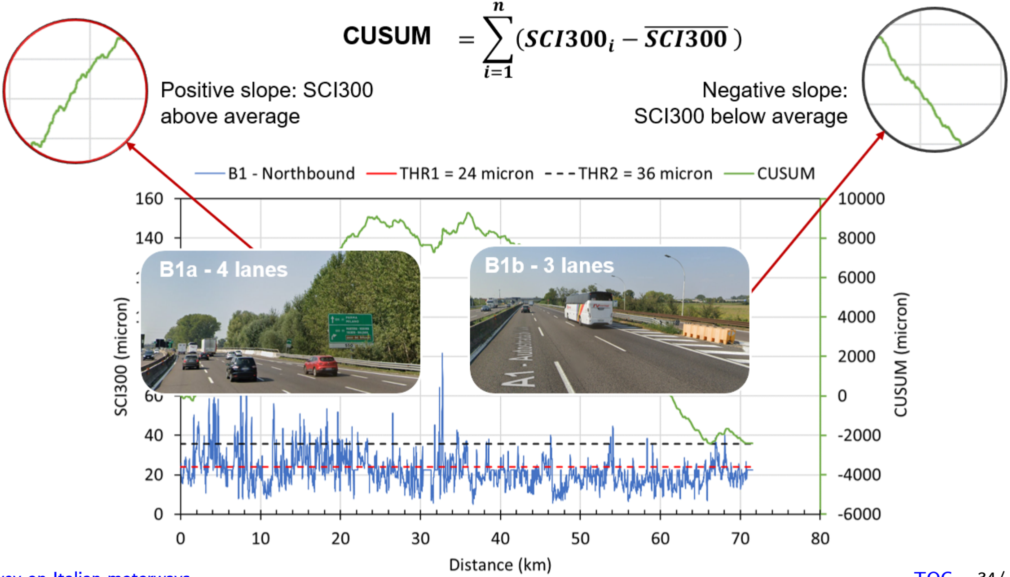

# A closer look at B1a data

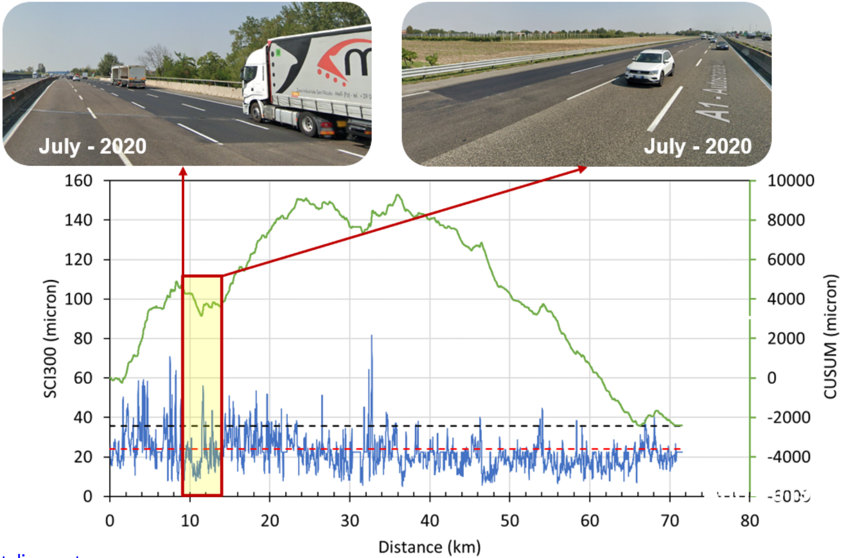

# Weak spots on B3 - southbound

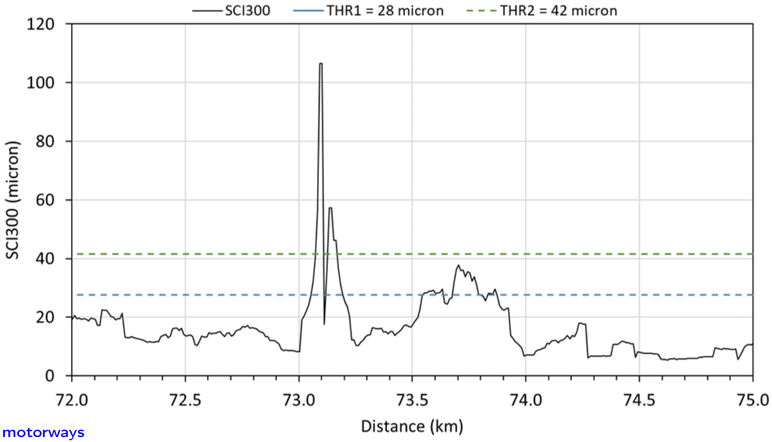

# Weak spots on B3 - southbound

# Bridges and viaducts

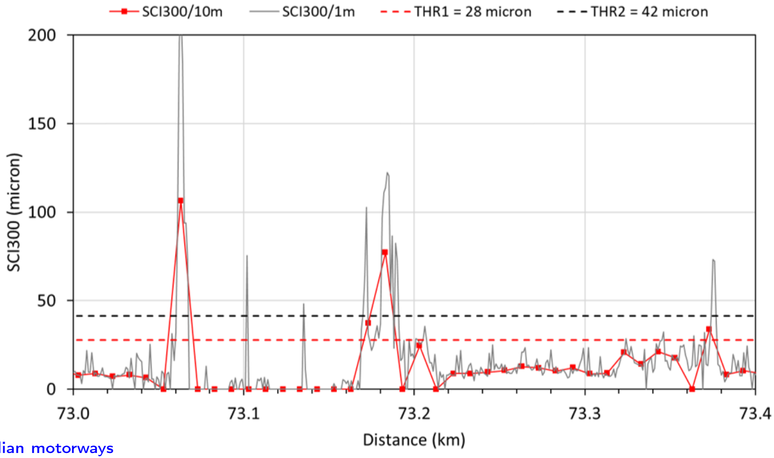

# Bridges and viaducts

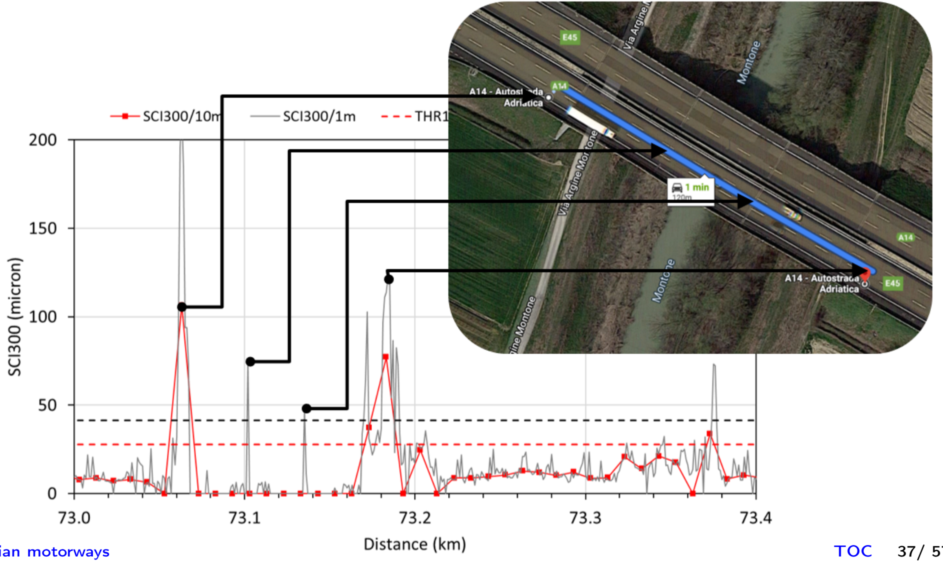

# Outline

# TSD for network-level management (Canestrari et al., 2022)

Our objective is to apply TSD measurements for network-level management of motorway pavements

Instead of using the SCI300 directly, we propose a methodology for estimating the remaining service life of the pavement

# TSD for network-level management (Canestrari et al., 2022)

Our objective is to apply TSD measurements for network-level management of motorway pavements

Instead of using the SCI300 directly, we propose a methodology for estimating the remaining service life of the pavement

Remaining service life is easier to manage at the network-level because it is easily understandable also by transportation executives and chief engineers

To be implementable within a network-level PMS, such methodology should be practical, realistic and easy to calibrate

# Main steps of the new methodology

0. divide the motorway network into sections of appropriate length

# Main steps of the new methodology

0. divide the motorway network into sections of appropriate length
1. normalize the measured SCI300 values to consider the variability of the applied load
2. adjust the normalised SCI300 considering pavement temperature

# Main steps of the new methodology

0. divide the motorway network into sections of appropriate length
1. normalize the measured SCI300 values to consider the variability of the applied load
2. adjust the normalised SCI300 considering pavement temperature

Then, for each section,

3. select a representative SCI300 value
4. estimate the remaining fatigue life considering bottom-up cracking as the critical distress
5. calculate the remaining service life as the ratio between the remaining fatigue life and the expected traffic

# 0. Divide the motorway network into sections

The length of the sections is established based on the local practices of the managing Authority

# 0. Divide the motorway network into sections

The length of the sections is established based on the local practices of the managing Authority

For Italian motorways:

- due to the high-traffic volumes, M&R activities must be carried out at night for safety reasons and to avoid traffic inconvenience. This means that the sections cannot be too long to allow re-opening to traffic before the morning peak
- on the other hand, intervening on too short sections would be uneconomical

# 0. Divide the motorway network into sections

The length of the sections is established based on the local practices of the managing Authority

For Italian motorways:

- due to the high-traffic volumes, M&R activities must be carried out at night for safety reasons and to avoid traffic inconvenience. This means that the sections cannot be too long to allow re-opening to traffic before the morning peak
- on the other hand, intervening on too short sections would be uneconomical

We used a section length of 500 m, but a different value (150 m, 250 m) can be used

Sections of different length have been implemented by ASPI in the newly developed E-PMS

The actual load applied on the measuring side (right) may be different from 50 kN

| | A | B | C | D |
|---|---|---|---|---|
| 1 | Distance [m] | Speed [Km/h] | Applied Load - Left [Kg] | Applied Load - RIght [Kg] |
| 2 | 0 | 23.9568 | 4282.7298 | 6324.2173 |
| 3 | 10 | 23.9054 | 4341.3683 | 6318.9825 |
| 4 | 20 | 23.8442 | 4205.0945 | 6322.1242 |

$$SCI300 = SCI300_{meas} \cdot \frac{50}{F_{right}} \tag{1}$$

# 2. Adjust $SCI300$ to the same reference temperature

For adjusting $SCI300$ values measured at various temperatures to a single reference temperature $T_r$, we used the model proposed by Nasimifar et al., 2020

$$SCI300_r = SCI300 \cdot \lambda \tag{2}$$

with:

$$\lambda = \frac{10^{-0.0521 \cdot T_r + 0.0322 \cdot T_r \cdot \log(h_{AC})}}{10^{-0.0521 \cdot T_f + 0.0322 \cdot T_f \cdot \log(h_{AC})}}$$

where:

- $T_r$ is the reference temperature (we used 20 °C)
- $T_f$ is the temperature at $h_{AC}/2$, estimated from the temperature of the pavement surface (measured by the TSD) using the BELLS3 model(⋆) (Lukanen et al., 2000)
- $h_{AC}$ is the thickness of the asphalt layers (we used the typical values given above, 290 or 250 mm)

# 3. Select a representative SCI300 value for each section

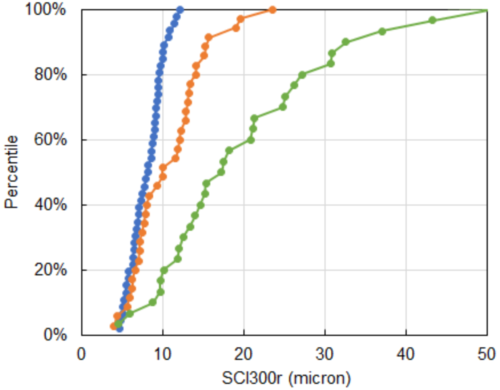


We based our selection criteria on the Empirical Cumulative Distribution (ECD) of $SCI300_r$ in each section

# 3. Select a representative SCI300 value for each section

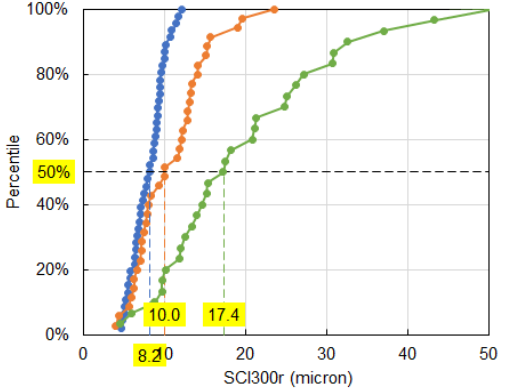


We based our selection criteria on the Empirical Cumulative Distribution (ECD) of $SCI300_r$ in each section

the 50th percentile (the median) would not be a conservative choice, because about half of the section would have higher deflections and thus worse conditions

# 3. Select a representative SCI300 value for each section

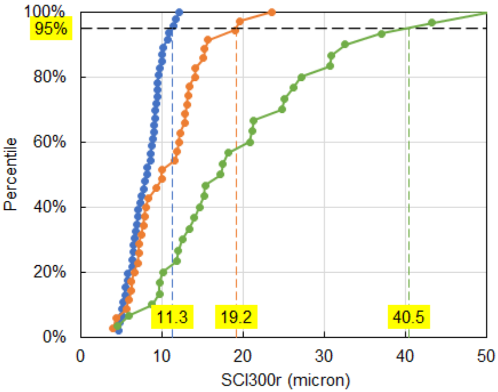


We based our selection criteria on the Empirical Cumulative Distribution (ECD) of $SCI300_r$ in each section

the 50th percentile (the median) would not be a conservative choice, because about half of the section would have higher deflections and thus worse conditions

the 95th percentile would be too conservative also because of the possible effect of outliers located in the tail of the ECD

# 3. Select a representative SCI300 value for each section

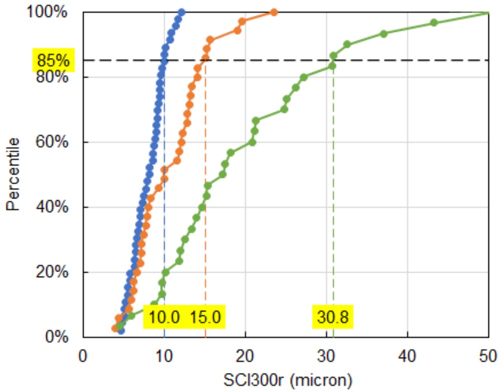


We based our selection criteria on the Empirical Cumulative Distribution (ECD) of $SCI300_r$ in each section

the 50th percentile (the median) would not be a conservative choice, because about half of the section would have higher deflections and thus worse conditions

the 95th percentile would be too conservative also because of the possible effect of outliers located in the tail of the ECD

the 85th percentile ($SCI300_{r,85}$) could be acceptable as initial choice, to be calibrated based on comparison between predicted and observed RSL

# 4. Estimate the residual fatigue life

For estimating the remaining fatigue life $N_f$ we used the classical model

$$N_f = f_1 \cdot \left(\frac{1}{\varepsilon_t}\right)^{f_2} \cdot \left(\frac{1}{E}\right)^{f_3} \tag{3}$$

where:

$\varepsilon_t$ is the maximum tensile strain at the bottom of the asphalt layers

$E$ stiffness of the asphalt layers

$f_1, f_2, f_3$ material fatigue coefficients (we used the AI values)

# 4. Estimate the residual fatigue life

We estimated the values of $\varepsilon_t$, and $E$ directly from the $SCI300_{r,85}$ using the relations proposed by Rada et al., 2016 and Nasimifar et al., 2020

$$\varepsilon^r_{t,max} = a \cdot (SCI300_{r,85})^b \tag{4}$$

$$E_r = c \cdot \left(\varepsilon^r_{t,max}\right)^d \tag{5}$$

where:

$a, b, c, d$ are coefficients that depend on the thickness of the asphalt layer (Nasimifar et al., 2020; Rada et al., 2016)

Substituting (4),(5) into (3), we obtain

$$N_{100}^{r} = \alpha\,(SCI300_{r,85})^{\beta} \qquad (6)$$

where

$SCI300_{r,85}$ is the representative $SCI300$ value of each section (at the reference temperature)

$N_{100}^{r}$ is the number of repetitions to fatigue failure, of 100 kN axles, at the reference temperature

$\alpha, \beta$ coefficients depending on the thickness of the pavement and the selected fatigue law

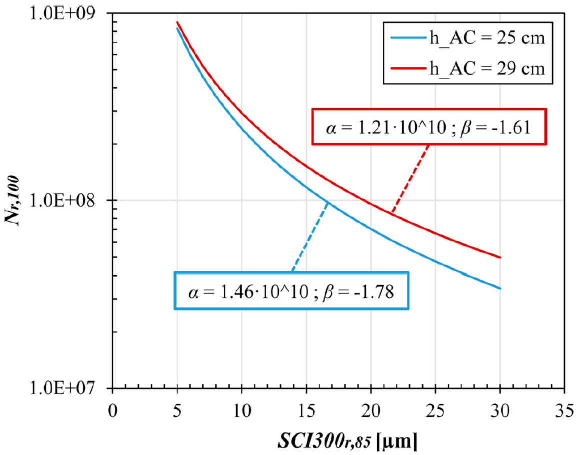

# Estimate the remaining service life

Finally we can express the structural capacity of each section in terms of remaining service life

$$RSL(\text{years}) = \frac{N_{100}^{r}}{N_0} \tag{7}$$

where:

$N_0$ annual traffic (100 kN ESALs)

Expressing the structural capacity in "years" is extremely important in a network-level perspective because it is clearly understandable also to budget directors and top officials

# Example application to B1

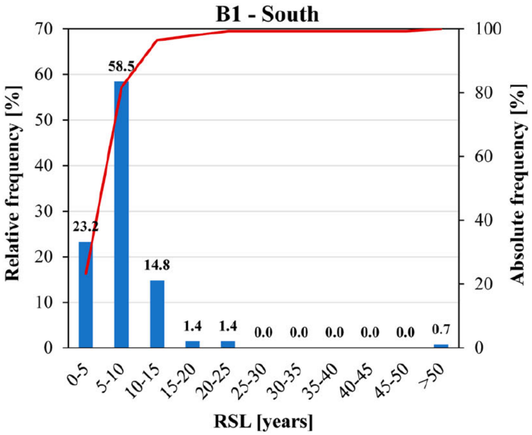


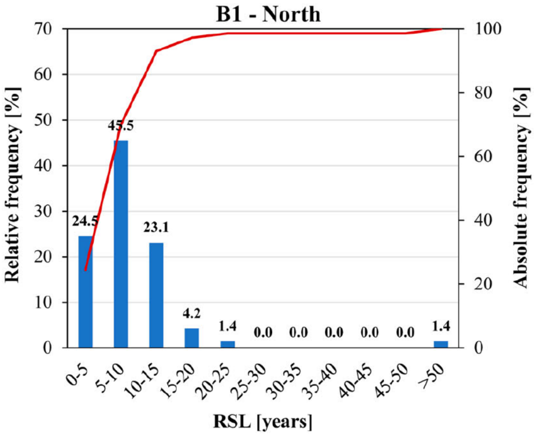

# Example application to B3

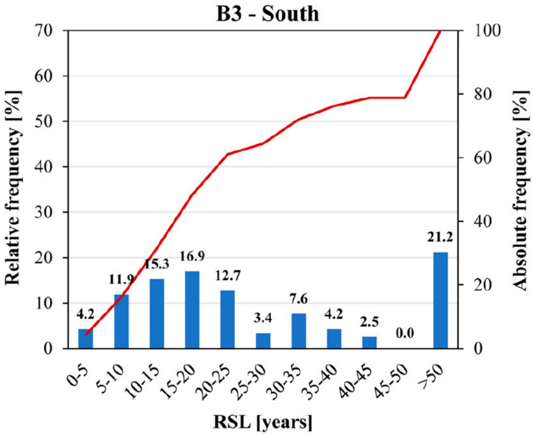


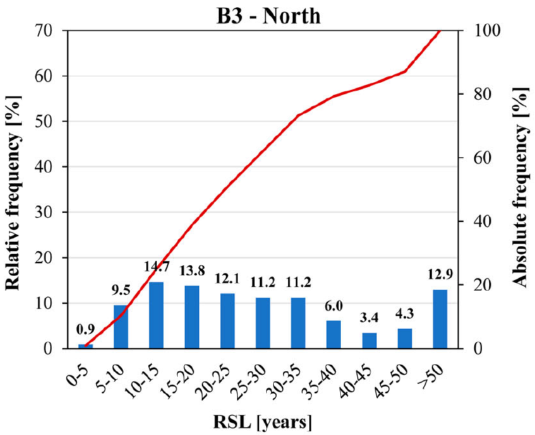

# Outline

# Final thoughts

1. understand pavement mechanics $\Rightarrow$ perform (deflection) measurements that allow predicting critical pavement responses
2. measure (deflections) accurately and precisely
3. adjust for measurement variability (e.g. temperature)
4. derive meaningful structural adequacy parameters the allow reliable budges decision

# Final thoughts

1. understand pavement mechanics $\Rightarrow$ perform (deflection) measurements that allow predicting critical pavement responses
2. measure (deflections) accurately and precisely
3. adjust for measurement variability (e.g. temperature)
4. derive meaningful structural adequacy parameters the allow reliable budges decision

The TSD is a young equipment and additional work is needed for improving in steps 2. and 3.

Additional measurement with embedded sensors, data science and artificial intelligence tools will be useful for improving in steps 2. and 3.

# Final thoughts

1. understand pavement mechanics ⇒ perform (deflection) measurements that allow predicting critical pavement responses
2. measure (deflections) accurately and precisely
3. adjust for measurement variability (e.g. temperature)
4. derive meaningful structural adequacy parameters the allow reliable budges decision

The TSD is a young equipment and additional work is needed for improving in steps 2. and 3.

Additional measurement with embedded sensors, data science and artificial intelligence tools will be useful for improving in steps 2. and 3.

Young researchers are needed or improving in steps 1 to 5!

# Thank you

add group photo, when available...

# References I


Baltzer, S. (2009). Three years of high speed deflectograph measurements of the danish state road network. *Bearing Capacity of Roads, Railways and Airfields. 8th International Conference (BCR2A'09) University of Illinois, Urbana-Champaign.*

Bland, J. M., & Altman, D. (1986). Statistical methods for assessing agreement between two methods of clinical measurement. *The lancet*, *327*(8476), 307–310.

Bodin, D., Zhalejoo, N., & Garton, D. (2019). *Improved methods of using pavement deflection data in the design of rehabilitation treatments* (Report AP-T350-19). Austroads.

Canestrari, F., Ingrassia, L. P., Spinelli, P., & Graziani, A. (2022). A new methodology to assess the remaining service life of motorway pavements at the network level from traffic speed deflectometer measurements. *International Journal of Pavement Engineering*, 1–12.

Chiola, D., Carambia, B., Tozzo, C., Gasbarro, N., & Spinelli, P. (2022). E-pms – evolutive pavement management system. *9th Symposium on Pavement Surface Characteristics SURF, Milano.*

Dias, K., Gravesen, J., Hjorth, P. G., Larsen, P., Please, C., Radulovic, N., Wang, L., & Aagaard, L. (2005). Beneath the wheel: Greenwood engineering. *54th European Study Group with Industry.*

Ferne, B. W., Langdale, P., Round, N., & Fairclough, R. (2009a). Development of a calibration procedure for the uk highways agency traffic-speed deflectometer. *Transportation research record.*

# References II


Ferne, B. W., Langdale, P., Round, N., & Fairclough, R. (2009b). Development of the uk highways agency traffic speed deflectometer. *Bearing Capacity of Roads, Railways and Airfields. 8th International Conference (BCR2A'09) University of Illinois, Urbana-Champaign*, 409–418.

Haas, R., & Hudson, W. R. (2015). *Pavement asset management*. John Wiley & Sons.

Hildebrand, G., & Rasmussen, S. (2002). *Development of a high speed deflectograph* (Report No. 117). Danish Road Institute.

Katicha, S. W., Flintsch, G. W., Ferne, B., & Bryce, J. (2014). Limits of agreement method for comparing tsd and fwd measurements. *International Journal of Pavement Engineering*, *15*(6), 532–541.

Kelley, J., & Moffat, M. (2012). *Review of the traffic speed deflectograph: Final project report* (Report AP-R395-12). Austroads.

Levenberg, E., Pettinari, M., Baltzer, S., & Christensen, B. M. L. (2018). Comparing traffic speed deflectometer and falling weight deflectometer data. *Transportation Research Record*, *2672*(40), 22–31.

Lukanen, E. O., Stubstad, R., Briggs, R. C., & Intertec, B. (2000). *Temperature predictions and adjustment factors for asphalt pavement* (tech. rep.). Turner-Fairbank Highway Research Center.

Molenaar, A. (2007). Prediction of fatigue cracking in asphalt pavements: Do we follow the right approach? *Transportation research record*, *2001*(1), 155–162.

Muller, W. B., & Roberts, J. (2013). Revised approach to assessing traffic speed deflectometer data and field validation of deflection bowl predictions. *International journal of pavement engineering*, *14*(4), 388–402.

# References III


Nasimifar, M., Chaudhari, S., Thyagarajan, S., & Sivaneswaran, N. (2020). Temperature adjustment of surface curvature index from traffic speed deflectometer measurements. *International Journal of Pavement Engineering*, *21*(11), 1408–1418.

Nasimifar, M., Thyagarajan, S., Chaudhari, S., & Sivaneswaran, N. (2019). Pavement structural capacity from traffic speed deflectometer for network level pavement management system application. *Transportation Research Record*, *2673*(2), 456–465.

Nasimifar, M., Thyagarajan, S., Siddharthan, R. V., & Sivaneswaran, N. (2016). Robust deflection indices from traffic-speed deflectometer measurements to predict critical pavement responses for network-level pavement management system application. *Journal of Transportation Engineering*, *142*(3), 04016004.

Nielsen, C. P. (2019). Visco-elastic back-calculation of traffic speed deflectometer measurements. *Transportation research record*, *2673*(12), 439–448.

Pedersen, L. (2013). Viscoelastic modelling of road deflections for use with the traffic speed deflectometer.

Pettinari, M., Baltzer, S., Kalantari, M., & Jansen, D. (2021). Development of simplified models to assess pavement structural condition on network level. *Eleventh International Conference on the Bearing Capacity of Roads, Railways and Airfields, Volume 1*, 288–298.

Rada, G. R., Nazarian, S., Visintine, B. A., Siddharthan, R. V., Thyagarajan, S., et al. (2016). *Pavement structural evaluation at the network level* (Publication FHWA-HRT-15-074). Federal Highway Administration.

Rasmussen, S., Aagaard, L., Baltzer, S., & Krarup, J. (2008). A comparison of two years of network level measurements with the traffic speed deflectometer. *Transport Research Arena.*

Roberts, J., Ai, U., Toole, T., & Martin, T. (2014). *Traffic speed deflectometer: Data review and lessons learnt* (Report AP-T279-14). Austroads.

Shrestha, S., Katicha, S. W., Flintsch, G. W., & Thyagarajan, S. (2018). Application of traffic speed deflectometer for network-level pavement management. *Transportation research record*, *2672*(40), 348–359.

Zihan, Z. U., Elseifi, M. A., Gaspard, K., & Zhang, Z. (2018). Development of a structural capacity prediction model based on traffic speed deflectometer measurements. *Transportation research record*, *2672*(40), 315–325.

Zihan, Z. U., Elseifi, M. A., Gaspard, K., & Zhang, Z. (2019). Relationship between surface-measured indices and in-service pavement structural conditions predicted from traffic speed deflection devices. *Transportation Research Record*, *2673*(2), 593–604.

Zofka, A., Sudyka, J., Maliszewski, M., Harasim, P., & Sybilski, D. (2014). Alternative approach for interpreting traffic speed deflectometer results. *Transportation Research Record*, *2457*(1), 12–18.